Rotational Solid Friction of a Nematic Liquid Crystal

Christophe Blanc, Mathieu Nespoulous,* Emmanuel Angot, and Maurizio Nobili

Laboratoire des Colloïdes, Verres et Nanomatériaux (LCVN), UMR5587 CNRS and Université Montpellier II, Place Eugène Bataillon, 34095 Montpellier, France

(Received 18 December 2009; revised manuscript received 28 July 2010; published 14 September 2010)

Liquid crystal defects are used as probes to study the local reorientation dynamics of the nematic surface director on SiO_x alignment layers. The tracking of the defect's motion reveals the presence of solid friction forces, unexpected in this complex viscous fluid. We identify the director pinning due to a surface quenched disorder as a possible mechanism that gives rise to the measured solid friction.

DOI: 10.1103/PhysRevLett.105.127801 PACS numbers: 61.30.Jf, 61.30.Hn, 61.72.Cc, 83.50.Lh

The dynamics of two solids in contact relies on specific interactions and dissipation mechanisms localized at the interface. For a solid body sliding on a solid substrate the resistant force is given by the Coulomb's law stating that the friction force is independent from the relative velocity [1]. Its physical origin is still debated. In particular, pinning by disordered asperities of the contacts [2] and irreversible processes like plastic deformations [3] all play significant roles. The solid elasticity is also of importance since it conveys the surface forces to the solid bulk. The solid friction therefore emerges from the competition between driving forces, disorder, plasticity and elasticity. The case of simple fluids is different: despite the usual no-slip boundary conditions a force applied to the bulk always induces a viscous flow. A complex fluid might, however, present elastic properties and therefore could in principle support solid friction.

We focus here on nematic liquid crystals characterized by an orientational order along an average direction: the director $\mathbf{n}$. A rotational viscosity and elastic torques are related to this additional degree of freedom [4]. A rotational solid friction conveyed by elastic torques is therefore possible. It is, however, noticeable that only a few experimental works have focused on the liquid crystal surface orientational dynamics [5]. The surface director $\mathbf{n}_s$ is usually oriented along a fixed direction $\mathbf{n}_0$, the so-called anchoring easy axis. If an external torque is applied, $\mathbf{n}_s$ may depart from $\mathbf{n}_0$. The surface dynamics is then often described by the competition between the external torque, a restoring anchoring torque, and a viscous surface one [5–7]. Such a simple approach cannot, however, explain phenomena such as *gliding*, a *slow* reorientation of the easy axis observed under large elastic torques that dissipates the stored elastic energy [8]. This irreversible behavior is, in a sense, similar to the plastic deformation of the contacts between two solid bodies. The surface disorder could also be a source of rotational solid friction. This role has been rarely discussed [9] but even a weak disorder should strongly influence the surface reorientation dynamics [10].

In this Letter, we examine the orientation dynamics of the nematic director on silicon oxide, an extensively characterized alignment layer. This dynamics is monitored through macroscopic defects moving on the surface. A quantitative analysis unambiguously reveals the presence of solid friction forces, which are equivalent to a solid friction torque for the surface director. Led by the analogy with the solid-solid friction, sensitive to both interface disorder and plastic mechanisms, we discuss the respective roles of the easy-axis disorder and the ''plastic'' memorization effect on the measured dynamics.

We have chosen the well-documented 4-cyano-4'-n-pentylbiphenyl (5CB) nematic liquid crystal and SiO_x anchoring layer [11]. A nematic cell of typical thickness 10 μm is formed by assembling two 1 mm thick glass plates. A planar anchoring is previously induced on both plates by evaporating a 15 nm thick SiO_x layer [11,12] at oblique incidence (60°). The plates are assembled with parallel easy axes to obtain a uniform planar director orientation. Contrary to other deposition techniques such as polymer rubbing, SiO_x evaporation provides a rather homogeneous alignment layer down to the micron scale with only nanometer-scaled height undulations [11]. For 5CB, it gives a strong zenithal anchoring [13] but a much weaker azimuthal one [14], enabling the rotation of the director in the substrate plane. After filling, the cell is introduced in a hot stage (Instec STC200D, regulated at $\pm 0.1°$) and observed with a polarizing microscope equipped with a CCD camera (Pulnix TM-6703).

We examined the dynamics of π walls, characterized by a 180° azimuthal rotation of the director between two equivalent regions [Fig. 1(a)]. Such defects are easily obtained by cooling from the isotropic phase [15–17]. The walls either terminate in vertical $\pm 1/2$ disclinations [18] [Fig. 1(b)] or form closed loops [Fig. 1(c)] separating the director field into two distinct domains. Large diameter loops are motionless and are still observed after months, whereas smaller diameter ones slowly shrink and then vanish with increasing velocity [Fig. 2(a)]. The irregular morphology of initial loops rapidly evolves toward a circular shape during the first steps of relaxation. The quantitative tracking of the radius R with time [Fig. 2(b)] then reveals that the loop dynamics is accurately fitted [19] by

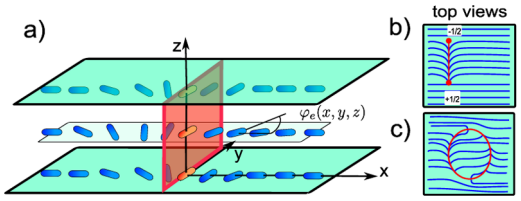

FIG. 1 (color online). (a) Sketch of the director field in a π wall. The azimuthal angle $\varphi_e(x, y, z)$ changes between 0 and π and gets $\pi/2$ at the center of the wall. The walls form either between two $\pm 1/2$ disclinations (b) or as closed loops (c). The surface director lines only are shown in the top views.

an affine law between the radial velocity $v = dR/dt$ and R^{-1}:

$$v \propto \frac{1}{R} - \frac{1}{R_c}, \tag{1}$$

R_c being a critical radius for which the loop is motionless.

The loops' shrinkage is formally equivalent to the disappearance of Bloch walls separating ferromagnetic domains of opposite magnetization. This analogy has already been used by Shenoy *et al.* [10] to examine the relaxation dynamics of reverse tilt loop domains in a nematic cell and compare them to Ising models that can include disorder. In the simplest uniform Ising model where a loop is viscously damped, the relaxation checks $v \propto R^{-1}$ [10] which clearly contradicts Eq. (1). Entering into a more quantitative approach, a π wall moves under the curvature-induced force $f_\gamma = \gamma/R$ where the line tension γ comes from both the bulk nematic elasticity and the anchoring energy. The line tension was computed from the equilibrium director orientation $\varphi_e(x, z)$ of a straight wall in Refs. [15,16]. Using here the one-constant approximation (single nematic elastic modulus K), and a Rapini-Papoular anchoring energy

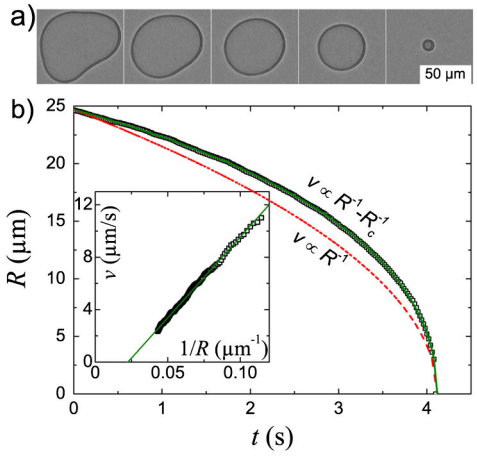

FIG. 2 (color online). Top: Relaxation of a π-wall loop observed between slightly uncrossed polarizers. Bottom and inset: the decreasing radius (open squares) of a circular loop with time is accurately fitted after integration of Eq. (1). The dependance $v \propto R^{-1}$ with the same initial and final points is also shown as a dashed curve. Error bars are smaller than the symbols.

[20] $W_a(\mathbf{n}_s, \mathbf{n}_0) = -(K/L)(\mathbf{n}_s.\mathbf{n}_0)^2$ (L is the azimuthal extrapolation length), it amounts to a value of order K:

$$\gamma = 2K\left[\frac{\pi}{2} - \arctan\left(\frac{L\pi}{d}\right) + \int_0^1 \frac{\arctan(\frac{d}{L\pi}t)}{t}dt\right], \tag{2}$$

where d is the cell thickness. A bulk drag force, at least, opposes the motion. It comes from the nematic orientational viscosity and can be computed in an adiabatic approximation from the dissipation occurring in a wall moving laterally along x, with a variation of the director azimuthal angle $\varphi(x, z, t) = \varphi_e(x - vt, z)$:

$$f_v = \frac{\gamma_1}{v}\iint\left(\frac{\partial\varphi}{\partial t}\right)^2 dxdz = \mu v, \tag{3}$$

where γ_1 is the rotational viscosity and the drag coefficient $\mu = \gamma_1 \iint(\partial\varphi_e/\partial x)^2 dxdz$ is independent from the velocity. The competition of the forces f_v and f_γ finally yields $v = \gamma/\mu R$. This dynamics is not observed but the data follow:

$$v = \frac{\gamma}{\mu}\left(\frac{1}{R} - \frac{1}{R_c}\right), \tag{4}$$

with a nearly constant slope γ/μ about 1.2×10^{-10} m^2/s in the $1\ \mu\text{m} < d < 20\ \mu\text{m}$ range [see Fig. 3(b)]. This value is compatible with typical data at 34 °C: $K = 4 \times 10^{-12}$ N, $L = 0.2\ \mu$m [21], $\gamma_1 = 0.034$ Pa · s [22]. The bulk dissipation therefore predominantly accounts for the wall *viscous* dissipation (this, however, does not exclude an additional weak surface viscous term).

More surprisingly, expression (4) reveals the presence of an additional force per unit length $f_c = \gamma/R_c$ acting as a solid friction force. When the local curvature radius R of the wall is larger than R_c, the line tension γ is too weak to displace the wall, pinned on the substrate. For $R < R_c$, the defect moves but two forces oppose the motion, the viscous force $f_v \propto v$ and a constant one f_c. We observe such a force in many other geometries including the stationary motion of elongated loops (detailed in Ref. [23]). This force ultimately originates from interactions between the substrate and the surface director. It defines a phenomenological solid friction torque per unit area τ opposing its rotation. When the wall moves a distance of Δx, the nonviscous energy dissipation ($f_c\Delta x$) is also the integrated energy dissipation of $\tau(\varphi)$ under the reorientation $\delta\varphi(x) = \Delta x\partial\varphi_e(x, 0)/\partial x$ on both surfaces. The mean friction torque per unit area is then $\langle\tau\rangle = f_c/2\pi$. For 5CB on SiO_x, its value is of order 10^{-7} N/m and it decreases rapidly [Fig. 3(a)] at the nematic to isotropic phase transition (35.3 °C). Note finally that the wall motion is smooth except near R_c where phenomena classically associated with solid friction such as stick-slip motions and avalanches are observed at the optical resolution limit. This suggests that the underlying mechanisms occur at this scale ($\approx$ 100 nm). We discuss now their possible origins and especially focus on the role of disorder which is commonly found to be at the origin of threshold forces for elastic media.

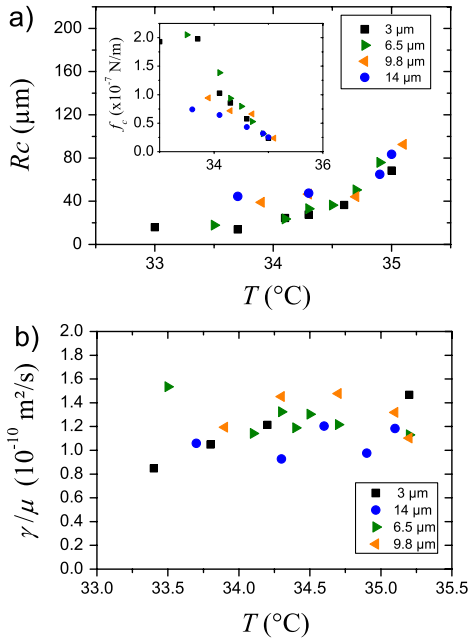

FIG. 3 (color online). Temperature dependance of the critical radius R_c (a), of the solid friction force (a; inset), and of the free energy-effective viscosity ratio γ/μ (b), for different sample thicknesses.

Such solid friction forces are indeed not restricted to the case of two bodies in contact but are also found in many other condensed matter systems such as the domain walls in thin magnetic films [24], the contact line of a liquid on a substrate [25–27] or the vortices in a superconductor [28]. Similarly, the measured force f_c can be seen as the pinning force acting on an elastic line in a disordered environment at the depinning threshold [29,30]. In the Ising model examined in Ref. [10], a disorder of random bond type (i.e., randomness in the local wall energy) is necessary to account for the coarsening dynamics of the tilt domains. In the SiO_x case, the randomness has to be related to the interface. Several types of disorder have already been evidenced in SiO_x layers. Structural TEM characterizations [11] have indeed revealed the presence of complex needle structures at the nanometer scale. At larger scale, a weak topographic disorder with nanometer height undulations has been characterized by atomic force microscopy up to the micron scale [31]. Whatever the exact nature of disorder, its influence on the surface director dynamics can be approached through the spatial heterogeneities of either the anchoring strength or the easy axis. Spatial heterogeneities of L are difficultly evidenced at the micron scale but a weak easy-axis disorder has been observed down to optical resolution [32] with a typical easy-axis angular standard deviation of 1°. It indicates that a quenched disorder of a few degrees of amplitude affects $\mathbf{n}_0$ at submicronic scale. Let us examine if such a disorder is compatible with a random bond disorder acting on the moving π wall.

For sake of simplicity, we consider the influence of a weak disorder along x characterized by an angular dispersion of the surface easy axis $\phi_0(x)$ identical on both substrates. Because of the disorder, a π wall centered in $x = x_0$ is slightly distorted and is now described by an azimuthal orientation $\varphi(x, z) = \varphi_e(x - x_0, z) + \delta\varphi(x, z)$. The free energy per unit length of the wall in the one-constant approximation is the sum of the bulk elastic energy and the surface Rapini-Papoular anchoring:

$$E_w = \int_V \frac{K}{2}(\nabla\varphi)^2 dv + \int_S \frac{K}{2L}\sin^2(\varphi - \phi_0) ds. \quad (5)$$

After a Taylor expansion on $\phi_0(x) \ll \pi$ and using the fact that $\varphi_e(x - x_0, z)$ minimizes E_w in absence of disorder, we obtain, at first order in $\phi_0(x)$:

$$E_w = \gamma + E_d + W_{w/d} \quad (6)$$

where E_d is the background free energy due to the disorder ϕ_0 and $W_{w/d}$ is a coupling term between the undistorted π wall and the disorder:

$$W_{w/d} = -\int \frac{K}{L}\sin\varphi_e(x - x_0)\cos\varphi_e(x - x_0)\phi_0(x) dx. \quad (7)$$

This coupling gives a force per unit length:

$$F_{w/d} = \int \frac{K}{L}\sin\varphi_e(x)\cos\varphi_e(x)\frac{\partial\phi_0(x + x_0)}{\partial x_0} dx. \quad (8)$$

These expressions simply show that a wall spontaneously settles on regions where $\cos\varphi_e$ and $\phi_0(x)$ are of the same sign (Fig. 4). The disorder thus creates loci made of anchoring energy traps and antitraps which pin the π wall in energy wells. An additional threshold force is then required to escape the potential wells and solid friction forces originate from the easy-axis heterogeneities.

As for other elastic systems such as domain walls in thin magnetic films [24] or the contact line of a liquid on a substrate [25–27], static and dynamic properties of the wall are governed by a complex competition between the bidimensional disorder that induces roughness and the elastic energy which tends to keep it locally straight. A further analysis, especially for collective pinning, will require a dedicated treatment. Simply note that the magnitude of the pinning force is given by Eq. (8) in the case of strong pinning, i.e., when the width of the wall at the surface (of order L [16]) is comparable to the size a of the traps. The yield force necessary to overcome the pinning is then $K\Delta\phi_0/a$ where $\Delta\phi_0$ is the amplitude of the easy-axis disorder. The magnitude obtained for $\Delta\phi_0 = 1°$,

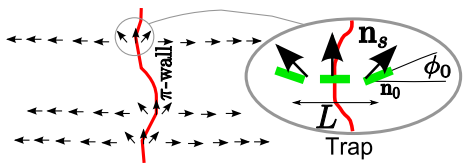

FIG. 4 (color online). In a weak easy-axis disorder, a π wall evolves in a complex energy landscape made of traps and antitraps depending on the local random easy-axis field.

$K = 4 \times 10^{-12}$ N and $L = 0.2$ μm, $F_{w/d} \approx 3.5 \times 10^{-7}$ N/m is comparable to the measured value f_c. Note finally that a similar analysis for a quenched disorder of anchoring strength gives $F_{w/d} \approx K\Delta L/L^2$ which has a similar magnitude for a disorder amplitude $\Delta L/L = 1\%$.

We have so far considered only the effect of elastic pinning on a quenched disorder. As in solid-solid friction [33], however, "plasticity" with nonviscous dissipation could also play an important role. We do not consider here a mechanical strain of the alignment layer under the nematic torque (unlikely for oxide) but an equivalent effect due to gliding. The easy-axis drift under the elastic torque indeed dissipates both the stored elastic and anchoring energy of the wall. In other words, gliding tends to trap the wall by adapting the local easy axis to the wall surface director and therefore reducing the driving force. The gliding appears at first sight to be negligible since the typical memorization time T_m on SiO_x layers is the hour [34] for a few degrees of reorientation. It is, however, necessary to compute the corresponding dissipation rate and compare it to the solid friction force dissipation rate $f_c v$. The stored energy of the wall being γ, an (upper) value of the dissipation rate due to gliding is γ/T_m. This term is independent from the wall velocity v and compares with $f_c v \approx \gamma v/R_c$ only for velocities $v \approx R_c/T_m$ at least 2 orders of magnitude lower than the observed ones. This observation rules out the surface memorization as the origin of the observed solid friction. The wall moves too fast for its distortion to be memorized. The memorization, however, probably plays an important role to reinforce the pinning of motionless loops of radius $R > R_c$ and definitely prevents any further creep motion at very long times.

To summarize, we have explored the reorientation dynamics of the surface director using the motion of macroscopic defects as probes. The π-wall dynamics unambiguously reveals the presence of a solid friction force. Differently from the usual solid-solid friction, the force is related to an orientational degree of freedom. It therefore defines a solid friction torque opposing the surface director rotation. This phenomenon cannot be explained by a slow drift of the easy axis (memorization effect), but is rather due to the presence of disorder in the easy-axis orientation or the anchoring strength. This work throws light on the neglected role of a weak disorder and the possibility to use pinning or depinning theories to approach complex liquid crystals surface dynamics.

*Present address: Institute of Industrial Science, University of Tokyo, 4-6-1 Komaba, Meguro-ku, Tokyo 153-8505, Japan.
math-nes@iis.u-tokyo.ac.jp

[1] C. A. Coulomb, *Théorie des Machines Simples* (Bachelier, Paris, 1821).
[2] J. B. Sokoloff, Phys. Rev. Lett. **86**, 3312 (2001).
[3] M. O. Robbins and M. H. Müser, in *Modern Tribology Handbook*, edited by B. Bhushan (CRC Press, Boca Raton, 2001).
[4] P. G. de Gennes and J. Prost, *The Physics Of Liquid Crystals* (Clarendon Press, Oxford, 1993).
[5] See G. Barbero and L. Pandolfi, Phys. Rev. E **79**, 051701 (2009) and references therein.
[6] B. Jérôme, P. C. Schuddeboom, and R. Meister, Europhys. Lett. **57**, 389 (2002).
[7] S. Faetti and M. Nobili, Phys. Lett. A **217**, 133 (1996).
[8] N. A. Clark, Phys. Rev. Lett. **55**, 292 (1985).
[9] L. Radzihovsky and Q. Zhang, Phys. Rev. Lett. **103**, 167802 (2009).
[10] D. K. Shenoy *et al.*, Phys. Rev. Lett. **82**, 1716 (1999).
[11] M. Monkade *et al.*, J. Phys. II (France) **7**, 1577 (1997).
[12] B. Jérôme, P. Piéranski, and M. Boix, Europhys. Lett. **5**, 693 (1988).
[13] H. Yokoyama, S. Kobayashi, and H. Kamei, J. Appl. Phys. **61**, 4501 (1987).
[14] S. Faetti *et al.*, Phys. Rev. Lett. **55**, 1681 (1985).
[15] A. Bogi *et al.*, Phys. Rev. Lett. **89**, 225501 (2002).
[16] C. Blanc *et al.*, Mol. Cryst. Liq. Cryst. **438**, 175 (2005).
[17] A. Vella *et al.*, Phys. Rev. E **71**, 061705 (2005).
[18] C. Blanc *et al.*, Phys. Rev. Lett. **95**, 097802 (2005).
[19] With notations of Eq. (4), after integration, the experimental points are fitted with $\frac{R}{R_c} + \ln(1 - \frac{R}{R_c}) = \frac{\gamma(t-t_f)}{\mu R_c^2}$.
[20] A. Rapini and M. Papoular, J. Phys. (Paris), Colloq. **30**, C4-54 (1969).
[21] M. Nobili *et al.*, Mol. Cryst. Liq. Cryst. **212**, 97 (1992).
[22] K. Skarp, S. T. Lagerwall, and B. Stebler, Mol. Cryst. Liq. Cryst. **60**, 215 (1980).
[23] See supplementary material at http://link.aps.org/supplemental/10.1103/PhysRevLett.105.127801.
[24] S. Lemerle *et al.*, Phys. Rev. Lett. **80**, 849 (1998).
[25] E. Rolley *et al.*, Phys. Rev. Lett. **80**, 2865 (1998).
[26] S. M. M. Ramos *et al.*, Phys. Rev. E **67**, 031604 (2003).
[27] A. Prevost, E. Rolley, and C. Guthmann, Phys. Rev. Lett. **83**, 348 (1999).
[28] A. I. Larkin and Yu. N. Ovchinikov, J. Low Temp. Phys. **34**, 409 (1979).
[29] See, for example, the reviews by D. S. Fisher, Phys. Rep. **301**, 113 (1998); S. Brazovskii and T. Nattermann, Adv. Phys. **53**, 177 (2004) and references therein.
[30] P. Chauve, T. Giamarchi, and P. Le Doussal, Phys. Rev. B **62**, 6241 (2000).
[31] R. Barberi *et al.*, J. Phys. Condens. Matter **6**, A275 (1994).
[32] M. Nespoulous, Ph.D. thesis, Université de Montpellier, 2008; M. Nespoulous, C. Blanc, and M. Nobili, Phys. Rev. Lett. **104**, 097801 (2010).
[33] T. Baumberger and C. Caroli, Adv. Phys. **55**, 279 (2006).
[34] S. Faetti, M. Nobili, and I. Raggi, Eur. Phys. J. B **11**, 445 (1999).